Progress In Electromagnetics Research, PIER 62, 49–68, 2006

NYSTRÖM METHOD WITH EDGE CONDITION FOR ELECTROMAGNETIC SCATTERING BY 2D OPEN STRUCTURES

M. S. Tong and W. C. Chew

Department of Electrical and Computer Engineering
University of Illinois, Urbana-Champaign (UIUC)
1406 West Green Street, Urbana, IL 61820, USA

Abstract—A Nyström method with edge condition (EC) is developed for electromagnetic scattering by two-dimensional (2D) open structures. Since EC correctly describes the edge behavior of currents on the scatterers, the use of it in Nyström method can dramatically coarsen the discretization near the edges. In the implementation of the scheme, we derive the closed-form expressions for the singular or near-singular integrations of Hankel functions multiplied by the polynomials with or without EC. This allows us to control the numerical errors efficiently by approximating the Hankel functions with more series terms and selecting higher-order polynomials to represent the currents in the local correction. The numerical results illustrate that the solutions with the use of EC converge much faster than without the use of EC. Also, EC is more essential in TM polarization than in TE polarization due to the singular behavior of current near edges.

1. INTRODUCTION

Nyström method has been used to solve for electromagnetic problems since 1990 [1]. The most distinguished feature of Nyström method is that it directly evaluates the integrands on quadrature points for the far-interaction terms in the impedance matrix without numerical integration. This advantage will greatly simplify the procedure for generating most terms in the impedance matrix. For the near-interaction terms which only account for a small portion in the matrix entries, the efficient local correction scheme is used [2, 3] and this will

result in a higher-order Nyström method at the cost of the moderate increase of complexity.

Compared with the method of moments (MoM) and other numerical algorithms, the Nyström method uses more unknowns for same geometrical discretization. This is because there are P unknowns on each cell, where P is the number of the quadrature points for a given quadrature rule. But the higher-order scheme can reduce the total number of unknowns to a level below MoM by coarsening the discretization if the same accuracy is concerned.

For the open structures, the sharp edges at the boundary of an open surface give rise to singular solutions. For low-order methods, the behavior of the singular solution can be captured by refining the mesh in the neighborhood of the singularity. However, higher-order methods usually do not converge well near the singularity, unless the singularity due to the edge condition (EC) is accounted for. We describe here a higher-order Nyström method (quadratic) whereby EC is accounted for. Since EC correctly reflects the current behavior near geometrical edges, the use of it allows one to dramatically coarsen the discretization near the edges without loss of accuracy.

The behavior of electromagnetic fields near an edge was first studied by Bouwkamp [4] and the so-called edge condition (EC) was named by his study. EC states that the electromagnetic energy density must be integrable over any finite domain even if this domain contains singularities of the electromagnetic field [5]. This condition requires that the tangential component of current be of the order $\rho^{-1/2}$, where ρ is the distance from the edge, while the normal component be of the order $\rho^{1/2}$. EC has been taken into account in many applications based on MoM [6, 7], but has not been incorporated into Nyström method yet. Also no higher-order methods using EC were found in the literature. As the first step, we study the function of EC in Nyström method for electromagnetic scattering by 2D conducting open scatterers. Both TM_z and TE_z polarizations are considered. The three-dimensional (3D) cases will be addressed in our future work.

The scattering by 2D open structures has been studied early using MoM without incorporating EC [8]. To investigate the function of EC in Nyström method, we need to coarsen the discretization extremely near edges. This will require to use more terms in the approximation of the singular kernel which is the zeroth-order Hankel function in TM case, and zeroth- and second-order Hankel functions in TE case. To this end, we derive the closed-form formulas for the integration of the singular kernel with arbitrary-term approximation multiplied by polynomials with or without EC. Although there are simpler series approximation formulas for singular kernels (for instance, 9.4.1–9.4.3

in [9]), we use the original series definition for them to emphasize the approximation accuracy. The polynomials are used to represent the currents over a self or near segment in the local correction. The higher-order polynomials will generate higher-order convergence rate when other numerical errors are negligible. It is demonstrated by our numerical experiments that if EC is used, the numerical solutions will converge much faster than without using EC. In addition, the use of EC is more significant in TM polarization than in TE polarization due to the singular behavior of TM currents near edges. The numerical errors for TM currents may be uncontrollable without using EC.

2. NYSTRÖM METHOD WITH EDGE CONDITION

Consider the electromagnetic scattering by a 2D conducting strip sketched in Fig. 1. The electric field integral equation (EFIE) to solve for this problem can be written as [8] (assuming $e^{-i\omega t}$ time dependence)

$$\begin{aligned} \frac{\kappa\eta}{4}\int_0^w J_z(x')H_0^{(1)}(\kappa\rho)dx' &= e^{-i\kappa x\cos\phi_i}, \\ \frac{\kappa\eta}{8}\int_0^w J_x(x')\left[H_0^{(1)}(\kappa\rho)+H_2^{(1)}(\kappa\rho)\cos 2\psi\right]dx' &= \sin\phi_i e^{-i\kappa x\cos\phi_i} \end{aligned} \tag{1}$$

where κ is the wave number, η is the intrinsic impedance, J_z and J_x are the induced currents along z and x direction corresponding to TM polarization and TE polarization respectively, and $H_0^{(1)}$ and $H_2^{(1)}$ are the zeroth-order and second-order Hankel functions of the first kind. $\rho = |x - x'|$ is the distance between a source point at x' and an observation point at x on the strip. The angles ϕ_i and ψ are defined

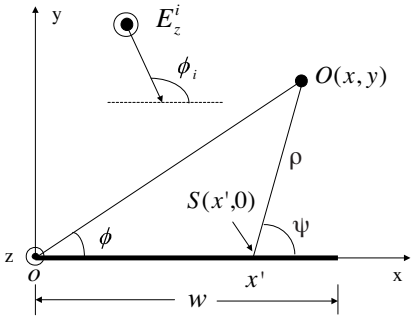

Figure 1. Geometry of scattering by a 2D conducting strip with a finite width.

in Fig. 1. To solve the EFIE's, we discretize the strip into N segments along x direction and the EFIE becomes

$$\sum_{i=1}^{N} \int_{x_i}^{x_{i+1}} J(x')g(x,x')dx' = V(x) \tag{2}$$

where $J(x')$ is either $J_z(x')$ (TM) or $J_x(x')$ (TE), $V(x)$ stands for the corresponding right-hand side, and $g(x,x')$ denotes the integral kernels in (1). Nyström method states that the integration over a segment can be replaced with a summation defined by a quadrature rule, i.e.,

$$I = \int_{x_i}^{x_{i+1}} J(x')g(x,x')dx' = \sum_{j=1}^{P} w_{(i,j)} g(x, x'_{(i,j)}) J_{(i,j)} \tag{3}$$

where P is the number of quadrature points, $w_{(i,j)}$ is the jth weight of a quadrature rule within the ith segment and $J_{(i,j)} = J(x'_{(i,j)})$ is the current value at the jth quadrature point within the ith segment. $J_{(i,j)}$ $(i = 1, \ldots, N;\ j = 1, \ldots, P)$ are also the unknowns we want to solve for in the matrix equation. We choose the Gaussian-Legendre quadrature rule for the integration in (3) for higher-order accuracy. However, the quadrature rule can only be applied when the integrand is smooth or the source point is far away from the observation point. If the source point coincides or approaches the observation point, the kernel is singular or near-singular and a local correction is needed. We have developed a simple higher-order local correction scheme for the scattering by 3D close structures [11]. This scheme can also be used for 2D open structures by incorporating EC. On the non-end self or near segments, the current is approximated using a polynomial, i.e.,

$$J^N(x') = \sum_{k=0}^{q} a_k x'^k \tag{4}$$

where q is the order of the polynomial and a_k $(k = 0, \ldots, q)$ are the coefficients. The superscript N implies the non-end segment and no subscript in J denotes that the approximation is valid for both TM and TE cases. For the self and near segments at two ends, EC is taken into account and the current is approximated as

$$J_z^L(x') = \frac{1}{\sqrt{x'}} \sum_{k=0}^{q} a_k x'^k$$

$$J_z^R(x') = \frac{1}{\sqrt{w - x'}} \sum_{k=0}^{q} a_k x'^k$$

$$J_x^L(x') = \sqrt{x'}\sum_{k=0}^{q} a_k x'^k$$
$$J_x^R(x') = \sqrt{w-x'}\sum_{k=0}^{q} a_k x'^k \tag{5}$$

where the subscripts z and x in J correspond to TM and TE polarizations, and the superscripts L and R correspond to the left ends and right ends, respectively. Since EC in (5) allows the approximation of the current to be much closer to the real current, we may dramatically coarsen the discretization and thus reduce the number of unknowns. The polynomial coefficients can be expressed into current values at the quadrature points by matching those current values at those quadrature points. This requires $q = P - 1$, i.e., the order of polynomial is one less than the number of quadrature points, to determine the coefficients uniquely. For $q = 1$ (linear approximation), the two-point quadrature rule is used and after determining those polynomial coefficients, the current can be written as

$$J^N(x') = \frac{(x_2'-x')J_1 + (x'-x_1')J_2}{x_2'-x_1'}$$
$$J_z^L(x') = \frac{\sqrt{x_1'}(x_2'-x')J_1 + \sqrt{x_2'}(x'-x_1')J_2}{\sqrt{x'}(x_2'-x_1')}$$
$$J_z^R(x') = \frac{\sqrt{w-x_1'}(x_2'-x')J_1 + \sqrt{w-x_2'}(x'-x_1')J_2}{\sqrt{w-x'}(x_2'-x_1')}$$
$$J_x^L(x') = \frac{\sqrt{x'}}{x_2'-x_1'}\left[\frac{x_2'-x'}{\sqrt{x_1'}}J_1 + \frac{x'-x_1'}{\sqrt{x_2'}}J_2\right]$$
$$J_x^R(x') = \frac{\sqrt{w-x'}}{x_2'-x_1'}\left[\frac{x_2'-x'}{\sqrt{w-x_1'}}J_1 + \frac{x'-x_1'}{\sqrt{w-x_2'}}J_2\right] \tag{6}$$

where x_1' and x_2' are the coordinates of the two quadrature points on each segment and J_1 and J_2 are the current values on those quadrature points. The current expressions using a quadratic approximation ($q = 2$) and three-point quadrature rule can be derived in a similar way. Substituting the above current approximation into the self and near segments in the discretized EFIE (2), we obtain

$$I^N = \sum_{k=0}^{q} J_{ik} \cdot \int_{x_i}^{x_{i+1}} a_k x'^k g(x,x')dx'$$

$$
\begin{aligned}
I_z^L &= \sum_{k=0}^{q} J_{ik} \cdot \int_{x_i}^{x_{i+1}} a_k x'^{k-0.5} g(x,x')dx' \\
I_z^R &= \sum_{k=0}^{q} J_{ik} \cdot \int_{x_i}^{x_{i+1}} \frac{a_k x'^{k}}{\sqrt{w-x'}} g(x,x')dx' \\
I_x^L &= \sum_{k=0}^{q} J_{ik} \cdot \int_{x_i}^{x_{i+1}} a_k x'^{k+0.5} g(x,x')dx' \\
I_x^R &= \sum_{k=0}^{q} J_{ik} \cdot \int_{x_i}^{x_{i+1}} a_k x'^{k} \sqrt{w-x'} g(x,x')dx'.
\end{aligned} \tag{7}
$$

In previous equations, we assume that the observation points are chosen arbitrarily on the strip. To create the matrix equation for the unknown currents on quadrature points, a point-matching process is needed by choosing the quadrature points as the observation points, i.e., $x = x'_{(m,n)}$ $(m = 1, \ldots, N;\ n = 1, \ldots, P)$. Once the observation points are chosen, the far, near and self segments can be defined accordingly. In the determination of matrix elements, the accurate evaluation of the integrations on the right-hand side of (7) is very critical. These integrations correspond to the diagonal and near-diagonal elements of the impedance matrix and their accuracy is tightly associated with the accuracy of solution. The other elements of the matrix, which reflect the far interactions between source points and observation points, are determined using (3) directly if the source points are not inside end segments. If the source points fall into end segments, numerical integrations are needed because the currents are expressed as the polynomials with EC. In this case, the Gaussian-Jacobi quadrature rule designed for the following integral is used [12]

$$
I = \int_{-1}^{1} (1-x)^{\alpha}(1+x)^{\beta} f(x)dx = \sum_{j=1}^{P} w_j f(x_j). \tag{8}
$$

We take $\alpha = -0.5$ (TM) or 0.5 (TE) and $\beta = 0$.

3. EVALUATION OF SINGULAR AND NEAR-SINGULAR INTEGRATIONS

Those integrals in (7) are singular or near-singular. For TM case, the kernel is the zeroth-order Hankel function including an integrable logarithmic singularity. The Lin-Log quadrature rule [13] has been designed to integrate such kind of integrands numerically. Nevertheless, analytical formulas are more desirable due to their

simplicity and flexibility in implementation. We derive such kind of closed-form expressions for those integrals based on the series approximation of the Hankel function. For TE case, the kernel possesses a hyper singularity in addition to the logarithmic singularity due to the appearance of the second-order Hankel function. In this case, the integral associated with the hyper-singular term is defined in a principal-value sense and the integration is performed by assuming that the observation point is initially located at a point (x_0, y_0) with $y_0 \neq 0$, and taking the $y_0 \to 0$ limit after finding the analytical expression for the integration [10]. Since we will use very coarse discretization to reach a higher-order accuracy, the commonly used small-argument approximation for the Hankel functions by taking the first series term [10] may not be accurate for us. For this reason, we derive the analytical formulas for the integration of Hankel functions with arbitrary-term approximation multiplied by a polynomial with or without EC.

3.1. TM Case

In the TM case, we need to perform the following three integrals found in (7)

$$\begin{aligned} I^N &= \int_{x_i}^{x_{i+1}} x'^k H_0^{(1)}(\kappa|x_0 - x'|)dx' \\ I^L &= \int_{x_i}^{x_{i+1}} x'^{k-0.5} H_0^{(1)}(\kappa|x_0 - x'|)dx' \\ I^R &= \int_{x_i}^{x_{i+1}} \frac{x'^k}{\sqrt{w - x'}} H_0^{(1)}(\kappa|x_0 - x'|)dx' \end{aligned} \tag{9}$$

where x_0 is the observation point falling into the integral interval (for self segments) or neighboring integral intervals (for near segments). The zeroth-order Hankel function can be expressed in a series form [9]

$$H_0^{(1)}(z) = \frac{i2}{\pi} \ln\left(\frac{z}{2}\right) \sum_{n=0}^{\infty} \frac{\left(-\frac{1}{4}z^2\right)^n}{(n!)^2} + \sum_{n=0}^{\infty} \left[1 - \frac{i2}{\pi}\psi(n+1)\right] \frac{\left(-\frac{1}{4}z^2\right)^n}{(n!)^2} \tag{10}$$

and the singularity comes from $\ln(\frac{z}{2})$ term. Note that the calculation of Hankel function by the series expansion is numerically inefficient when the argument is very large [14]. However, the argument is usually smaller than 15 because the above series only applies to the self and near interaction between a source point and an observation point and the series converges very fast. For example, the numerical error of

both zeroth-order and second-order Hankel functions will be below 10^{-10} when the number of terms in the series reaches 20 if $z = 15$. Substituting the series expansion for the Hankel function in (9), the singular parts of the integrals take the following form for the nth term

$$\begin{aligned}
I_s^N &= \int_{x_i}^{x_0} x'^k (x_0 - x')^{2n} \ln(x_0 - x') dx' \\
&\quad + \int_{x_0}^{x_{i+1}} x'^k (x' - x_0)^{2n} \ln(x' - x_0) dx' \\
I_s^L &= \int_{x_i}^{x_0} x'^{k-0.5} (x_0 - x')^{2n} \ln(x_0 - x') dx' \\
&\quad + \int_{x_0}^{x_{i+1}} x'^{k-0.5} (x' - x_0)^{2n} \ln(x' - x_0) dx' \\
I_s^R &= \int_{x_i}^{x_0} (w - x')^{-0.5} x'^k (x_0 - x')^{2n} \ln(x_0 - x') dx' \\
&\quad + \int_{x_0}^{x_{i+1}} (w - x')^{-0.5} x'^k (x' - x_0)^{2n} \ln(x' - x_0) dx' \qquad (11)
\end{aligned}$$

where the subscript s means the singular part. With the aid of (610.9) and (621.9) in [15], we can derive the following closed-form expressions for these integrals

$$\begin{aligned}
I_s^N &= \sum_{p=0}^{k} C_k^p x_0^p \left[(-1)^p \frac{\delta_1^\ell}{\ell} (\ln \delta_1 - 1/\ell) + \frac{\delta_2^\ell}{\ell} (\ln \delta_2 - 1/\ell) \right] \\
I_s^L &= \sum_{p=0}^{2n} C_{2n}^p x_0^{2n-p} \ (-1)^p \frac{1}{u} \left(x_{i+1}^u \ln \delta_2 - x_i^u \ln \delta_1 + I_1^{(\alpha)} \right) \text{ with} \\
I_1^{(\alpha)} &= \frac{1}{u} \left(x_i^u - x_{i+1}^u \right) + x_0 I_1^{(\alpha-1)} \text{ and} \\
I_1^{(0)} &= 2 \left(\sqrt{x_i} - \sqrt{x_{i+1}} \right) + \sqrt{x_0} \left(\ln \left| \frac{\sqrt{x_i} - \sqrt{x_0}}{\sqrt{x_i} + \sqrt{x_0}} \right| - \ln \left| \frac{\sqrt{x_{i+1}} - \sqrt{x_0}}{\sqrt{x_{i+1}} + \sqrt{x_0}} \right| \right) \\
I_s^R &= \sum_{p=0}^{2n} \sum_{r=0}^{k} C_{2n}^p C_k^r t_0^{4n-2p} (-1)^\beta w^{k-r} \frac{2}{v} \left(t_1^v \ln \delta_1 - t_2^v \ln \delta_2 + I_2^{(\beta)} \right) \text{ with} \\
I_2^{(\beta)} &= \frac{2}{v} \left(t_2^v - t_1^v \right) + t_0^2 I_2^{(\beta-1)} \text{ and} \\
I_2^{(0)} &= 2(t_2 - t_1) + t_0 \left(\ln \left| \frac{t_2 - t_0}{t_2 + t_0} \right| - \ln \left| \frac{t_1 - t_0}{t_1 + t_0} \right| \right) \qquad (12)
\end{aligned}$$

where $\ell = 2n + k + 1 - p$, $\delta_1 = x_0 - x_i$, $\delta_2 = x_{i+1} - x_0$, $u = p + k + 0.5$, $\alpha = p + k$, $v = 2(p + r) + 1$, $\beta = p + r$, $t_0 =$

$\sqrt{w-x_0}$, $t_1=\sqrt{w-x_i}$, $t_2=\sqrt{w-x_{i+1}}$ and C_{2n}^p or C_k^r is the binomial expansion coefficients. The non-singular part of the Hankel function is a polynomial and the integration with this part in (9) can be easily derived. For the integrations over near segments in (9), there is no singularity in the kernel and the corresponding formulas can be derived in a similar way.

3.2. TE Case

In the TE case, the singular and near-singular integrations consist of two parts. The first part includes the zeroth-order Hankel function kernel as shown in (10) and the singular integrals can be expressed as

$$\begin{aligned}
I_s^N &= \int_{x_i}^{x_0} x'^k (x_0-x')^{2n}\ln(x_0-x')dx' \\
&\quad + \int_{x_0}^{x_{i+1}} x'^k (x'-x_0)^{2n}\ln(x'-x_0)dx' \\
I_s^L &= \int_{x_i}^{x_0} x'^{k+0.5} (x_0-x')^{2n}\ln(x_0-x')dx' \\
&\quad + \int_{x_0}^{x_{i+1}} x'^{k+0.5} (x'-x_0)^{2n}\ln(x'-x_0)dx' \\
I_s^R &= \int_{x_i}^{x_0} \sqrt{w-x'}\,x'^k (x_0-x')^{2n}\ln(x_0-x')dx' \\
&\quad + \int_{x_0}^{x_{i+1}} \sqrt{w-x'}\,x'^k (x'-x_0)^{2n}\ln(x'-x_0)dx'. \qquad (13)
\end{aligned}$$

The closed-form expressions for these integrals are the same as in (12) except for the following two formulas

$$\begin{aligned}
I_1^{(0)} &= \frac{2}{3}\left(x_i^{1.5}-x_{i+1}^{1.5}\right) + 2x_0\left(\sqrt{x_i}-\sqrt{x_{i+1}}\right) \\
&\quad + x_0^{1.5}\left(\ln\left|\frac{\sqrt{x_i}-\sqrt{x_0}}{\sqrt{x_i}+\sqrt{x_0}}\right| - \ln\left|\frac{\sqrt{x_{i+1}}-\sqrt{x_0}}{\sqrt{x_{i+1}}+\sqrt{x_0}}\right|\right) \\
I_2^{(0)} &= \frac{2}{3}\left(t_2^{1.5}-t_1^{1.5}\right) + 2t_0^2(t_2-t_1) \\
&\quad + t_0^{1.5}\left(\ln\left|\frac{t_2-t_0}{t_2+t_0}\right| - \ln\left|\frac{t_1-t_0}{t_1+t_0}\right|\right) \qquad (14)
\end{aligned}$$

with $u=p+k+1.5$ and $v=2(p+r)+3$.

The second part includes the second-order Hankel function kernel and the integrals take the following forms

$$I_s^N = \int_{x_i}^{x_{i+1}} x'^k H_2^{(1)}(\kappa|x_0-x'|)\cos 2\psi dx'$$

$$I_s^L = \int_{x_i}^{x_{i+1}} x'^{k+0.5} H_2^{(1)}(\kappa|x_0 - x'|)\cos 2\psi dx'$$
$$I_s^R = \int_{x_i}^{x_{i+1}} x'^{k}\sqrt{w - x'} H_2^{(1)}(\kappa|x_0 - x'|)\cos 2\psi dx'. \quad (15)$$

By checking the series expression of the second-order Hankel function [9]

$$H_2^{(1)}(z) = -\frac{i}{\pi} - \frac{i4}{\pi z^2} + \frac{i2}{\pi}\ln\left(\frac{z}{2}\right)\sum_{k=0}^{\infty}\frac{z^2\left(-\frac{1}{4}z^2\right)^k}{4k!(k+2)!}$$
$$+\sum_{k=0}^{\infty}\left\{1 - \frac{i}{k}[\psi(k+1) + \psi(k+3)]\right\}\frac{z^2\left(-\frac{1}{4}z^2\right)^k}{4k!(k+2)!} \quad (16)$$

we find that the singular integrations come from the terms including $\frac{1}{z^2}$ and $\ln(\frac{z}{2})$. For the integration associated with $\frac{1}{z^2}$, it is defined in a principal-value sense. We assume that the observation point is initially located at the point (x_0, y_0) with $y_0 \neq 0$, thus resulting in a non-singular integration. The original integration is the $y_0 \to 0$ limit of the non-singular integration. This can be written as

$$I_s^N = \lim_{y_0\to 0}\int_{x_i}^{x_{i+1}} \frac{x'^k}{(x_0 - x')^2 + y_0^2}\cos 2\psi dx'$$
$$= \lim_{y_0\to 0}\mathrm{Re}\left\{\int_{x_i}^{x_{i+1}} \frac{x'^k}{(z_0 - x')^2}dx'\right\}$$
$$I_s^L = \lim_{y_0\to 0}\int_{x_i}^{x_{i+1}} \frac{x'^{k+0.5}}{(x_0 - x')^2 + y_0^2}\cos 2\psi dx'$$
$$= \lim_{y_0\to 0}\mathrm{Re}\left\{\int_{x_i}^{x_{i+1}} \frac{x'^{k+0.5}}{(z_0 - x')^2}dx'\right\}$$
$$I_s^R = \lim_{y_0\to 0}\int_{x_i}^{x_{i+1}} \frac{x'^k\sqrt{w - x'}}{(x_0 - x')^2 + y_0^2}\cos 2\psi dx'$$
$$= \lim_{y_0\to 0}\mathrm{Re}\left\{\int_{x_i}^{x_{i+1}} \frac{x'^k\sqrt{w - x'}}{(z_0 - x')^2}dx'\right\} \quad (17)$$

where we have used

$$\cos 2\psi = \frac{(x_0 - x')^2 - y_0^2}{(x_0 - x')^2 + y_0^2} \quad (18)$$

and introduced a complex number $z_0 = x_0 + iy_0$ corresponding to the position of observation point on the complex plane. The integrals in (17) are all analytically integrable with the aid of (194.1.) and (194.2.) in [15]. For $k = 0, 1, 2$ we can derive (the subscript of I denotes the value of k)

$$\begin{aligned}
I_0^N &= -\left(\frac{1}{\delta_1} + \frac{1}{\delta_2}\right) \\
I_1^N &= \ln\left|\frac{\delta_2}{\delta_1}\right| - x_0\left(\frac{1}{\delta_1} + \frac{1}{\delta_2}\right) \\
I_2^N &= \delta_1 + \delta_2 + 2x_0 \ln\left|\frac{\delta_2}{\delta_1}\right| - x_0^2\left(\frac{1}{\delta_1} + \frac{1}{\delta_2}\right) \\
I_0^L &= \frac{r_3}{2\sqrt{x_0}} - \left(\frac{r_2}{\delta_2} + \frac{r_1}{\delta_1}\right) \\
I_1^L &= -\frac{1}{x_0}\left(\frac{r_2^5}{\delta_2} + \frac{r_1^5}{\delta_1}\right) + \frac{r_2^3 - r_1^3}{x_0} + 3(r_2 - r_1) + \frac{3r_3\sqrt{x_0}}{2} \\
I_2^L &= -\frac{1}{x_0}\left(\frac{r_2^7}{\delta_2} + \frac{r_1^7}{\delta_1}\right) + \frac{r_2^5 - r_1^5}{x_0} + \frac{5}{3}\left(r_2^3 - r_1^3\right) \\
&\quad +5x_0(r_2 - r_1) + \frac{5x_0\sqrt{x_0}}{2}r_3 \\
I_0^R &= -\left(\frac{s_2}{\delta_2} + \frac{s_1}{\delta_1}\right) - \frac{s_3}{2s_0} \\
I_1^R &= 2(s_2 - s_1) + s_0 s_3 + x_0 I_0^R \\
I_2^R &= -\frac{2}{3}\left(s_2^3 - s_1^3\right) + 2x_0 I_1^R + x_0^2 I_0^R
\end{aligned} \tag{19}$$

where

$$\begin{aligned}
r_1 &= \sqrt{x_0 - \delta_1} \\
r_2 &= \sqrt{x_0 + \delta_2} \\
r_3 &= \ln\left|\frac{r_2 - \sqrt{x_0}}{r_2 + \sqrt{x_0}}\right| - \ln\left|\frac{r_1 - \sqrt{x_0}}{r_1 + \sqrt{x_0}}\right| \\
s_0 &= \sqrt{w - x_0} \\
s_1 &= \sqrt{w - x_0 + \delta_1} \\
s_2 &= \sqrt{w - x_0 - \delta_2} \\
s_3 &= \ln\left|\frac{s_2 - s_0}{s_2 + s_0}\right| - \ln\left|\frac{s_1 - s_0}{s_1 + s_0}\right|.
\end{aligned} \tag{20}$$

For the integrations associated with $\ln(\frac{z}{2})$ term, the observation points

are chosen on the strip directly and $\cos 2\psi = 1$, so they can be written as

$$\begin{aligned} I_s^N &= \int_{x_i}^{x_{i+1}} x'^k (x_0 - x')^{2n+2} \ln|x_0 - x'| dx' \\ I_s^L &= \int_{x_i}^{x_{i+1}} x'^{k+0.5} (x_0 - x')^{2n+2} \ln|x_0 - x'| dx' \\ I_s^R &= \int_{x_i}^{x_{i+1}} \sqrt{w - x'} x'^k (x_0 - x')^{2n+2} \ln|x_0 - x'| dx' \end{aligned} \tag{21}$$

and the corresponding formulas are obtained by replacing $2n$ with $2n + 2$ in (13). For integrations over near segments, there is no singularity and $\cos 2\psi = 1$, and all formulas can be derived in a similar way.

4. NUMERICAL RESULTS

To check the function of EC in Nyström method, we take $w = 2\lambda$ and 5λ, where λ is the wavelength, and $\phi_i = 90°$ in Fig. 1 and solve for the current distributions on the strip surface for both TM and TE polarizations. Figs. 2–5 show the corresponding solutions with and

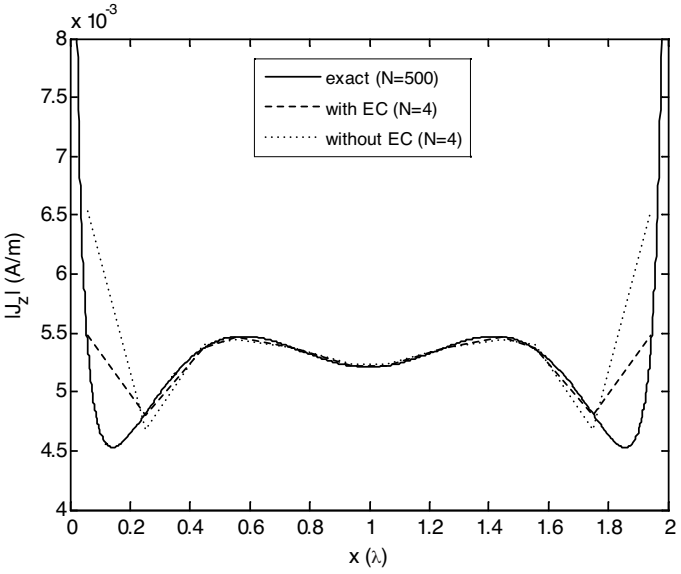

Figure 2. Current distribution on the strip for TM polarization, $w = 2\lambda$.

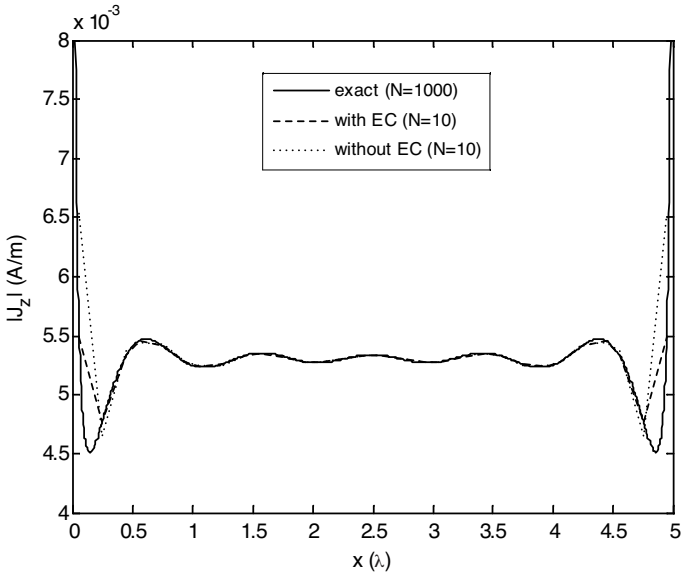

Figure 3. Current distribution on the strip for TM polarization, $w = 5\lambda$.

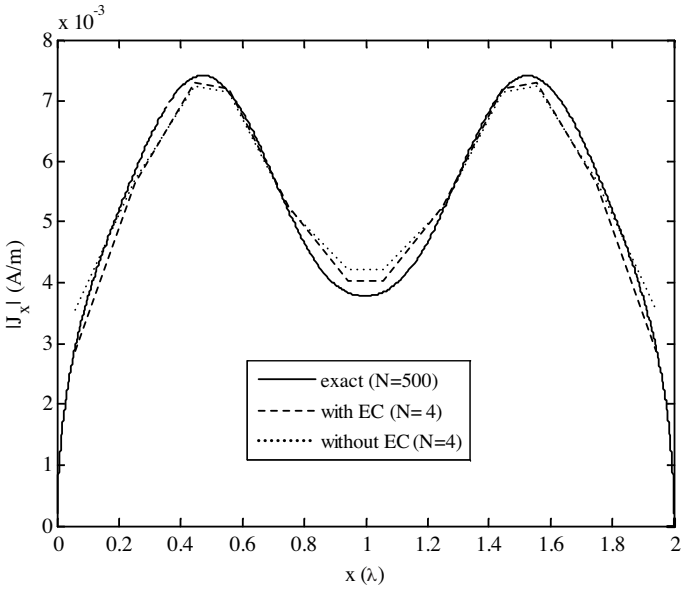

Figure 4. Current distribution on the strip for TE polarization, $w = 2\lambda$.

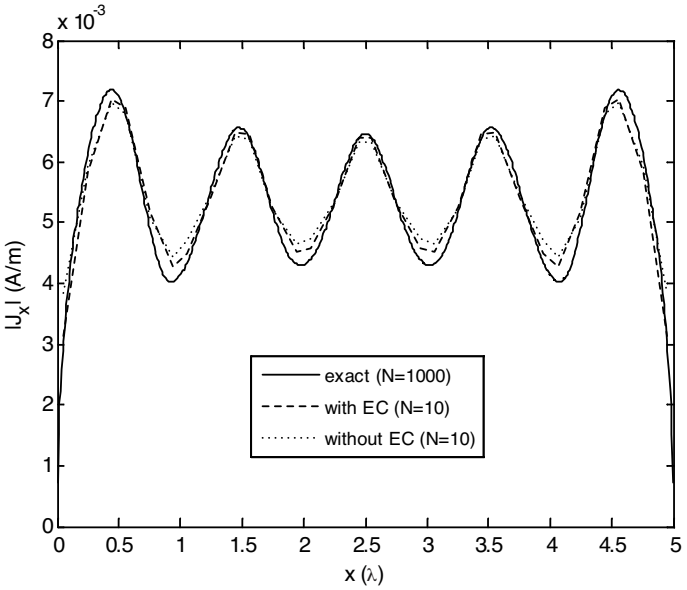

Figure 5. Current distribution on the strip for TE polarization, $w = 5\lambda$.

without EC based on a quadratic polynomial approximation ($q = 2$) for the currents in the local correction. The solutions when $N = 500$ for $w = 2\lambda$ and $N = 1000$ for $w = 5\lambda$ are stable enough and can be treated as exact solutions for comparison purpose (the root-mean-square (RMS) error will be below 10^{-8} when the mesh size decreases further). From these figures, we can see that the solutions with EC are much more accurate than without EC for the same discretization. Also, if we compare Fig. 4 with Fig. 2 in [10] for TE case with $w = 2\lambda$, our solutions with $N = 4$ are much better than those MoM solutions with $N = 20$. This fact indicates that higher-order Nyström method uses less unknowns than MoM.

Figs. 6 and 7 illustrate the current distribution obtained by interpolation using N = 10 and quadratic approximation. These solutions almost coincide with the exact solutions, indicating that the highly accurate current value at an arbitrary point can be achieved by interpolation even using very coarse discretization. The interpolation formulas are the polynomials (4) and (5) in the local correction scheme. Figs. 8–11 present the specific numerical errors for those solutions in terms of RMS error definition. In the comparison, the exact current values on non-quadrature points in the exact solutions are obtained

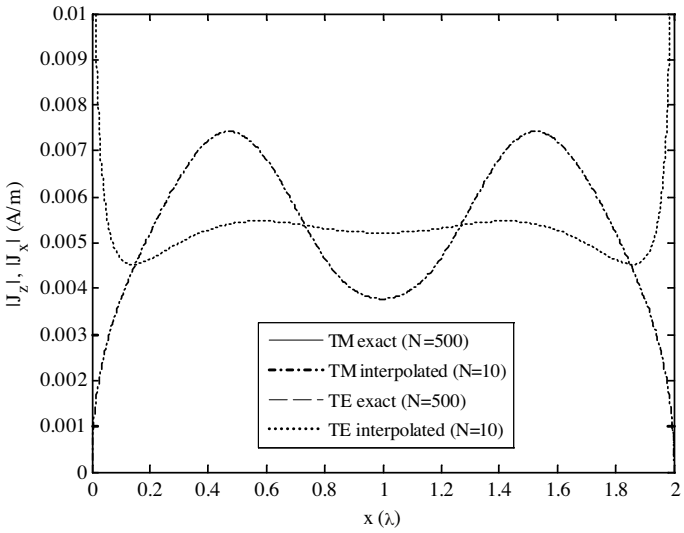

Figure 6. Interpolated current distribution using very coarse meshes, $w = 2\lambda$.

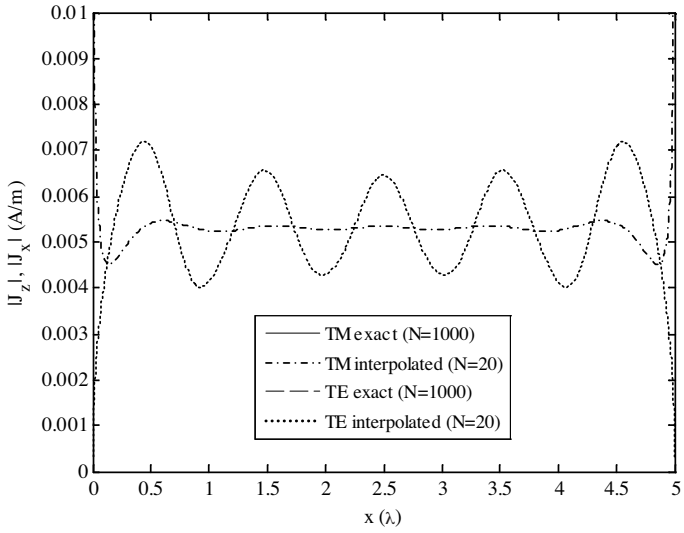

Figure 7. Interpolated current distribution using very coarse meshes, $w = 5\lambda$.

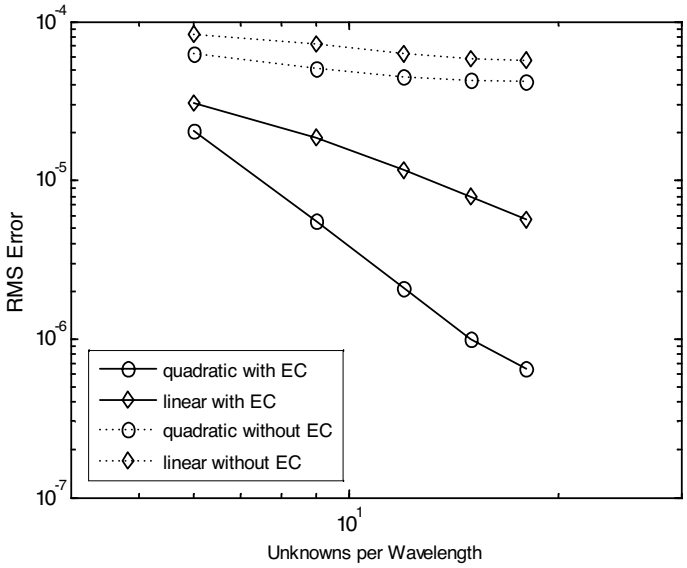

Figure 8. RMS error of the current for TM polarization, $w = 2\lambda$.

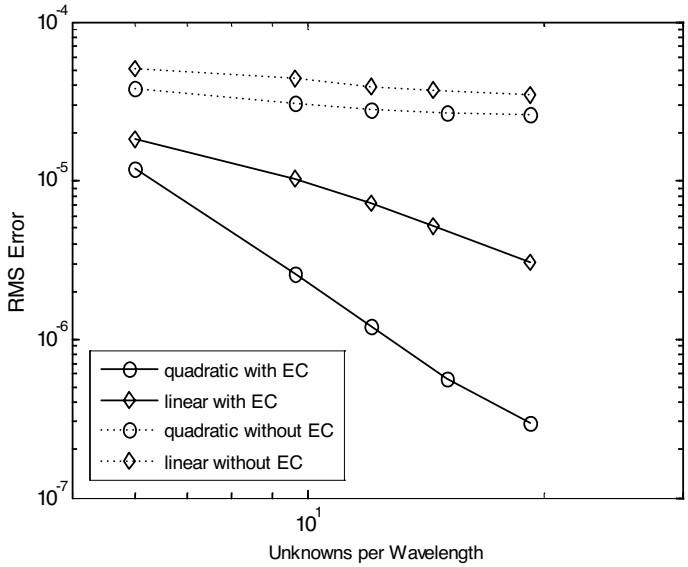

Figure 9. RMS error of the current for TM polarization, $w = 5\lambda$.

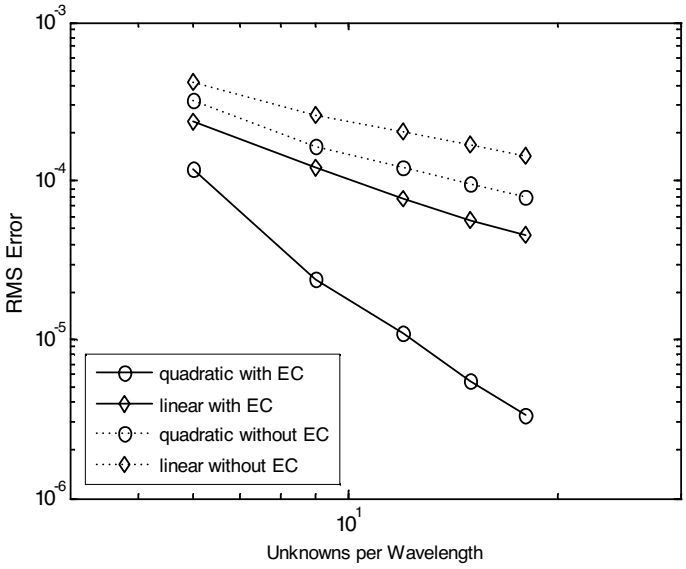

Figure 10. RMS error of the current for TE polarization, $w = 2\lambda$.

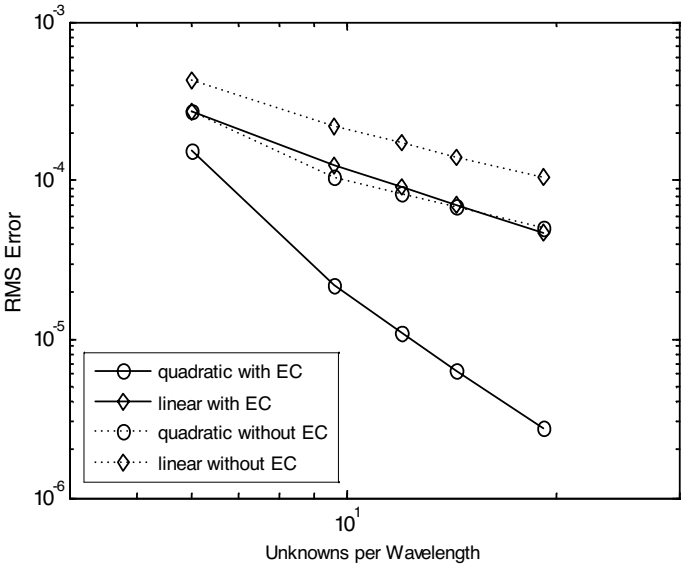

Figure 11. RMS error of the current for TE polarization, $w = 5\lambda$.

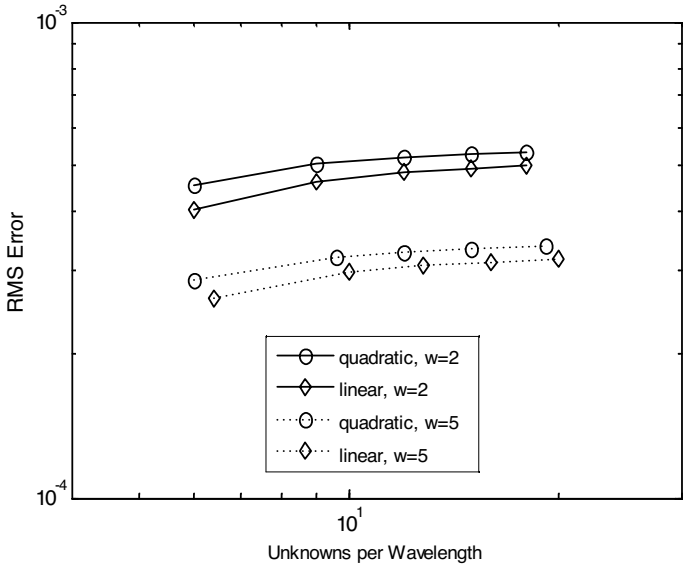

Figure 12. RMS error of the current for TM polarization without EC. Two end points are counted.

by the interpolation based on (4) and (5). These figures demonstrate that the solutions with EC converge much faster than without EC, especially for TM case. There is also an obvious p-refinement with the use of EC, i.e., a higher-order quadrature rule or higher-order polynomial approximation for the currents in the local correction yields a higher-order convergence rate. Note that we remove two end points in the calculation of errors for TM without-EC case. This is because the errors on these two points, if included, will dominate the total errors which increase slowly as the mesh size decreases. Fig. 12 depicts the numerical error curves for this case. This phenomenon reflects that the use of EC is more essential in TM case than in TE case and the numerical error may be uncontrollable without using EC in TM case. The reason for this is that the TM current is singular near edges and it is very easy to cause a large numerical error near edges without EC restriction. In the contrast, EC is not as essential in TE case because of the regular current behavior near edges. The solution can still converge fast without using EC, but apparently the use of EC can accelerate the convergence.

5. CONCLUSION

We develop the EC-based Nyström method for electromagnetic scattering by 2D open structures. EC allows us to coarsen the discretization dramatically. To enhance the accuracy to a higher order for very coarse meshes, we derive the closed-form formulations for the integrations of the kernels with arbitrary-term approximation multiplied by the polynomials with or without EC. Numerical results show that the application of EC will substantially enhance the convergence rate and a higher-order accuracy can be achieved with higher-order polynomial approximation in the local correction. Also, the use of EC is more essential in TM case than in TE case. The numerical error for TM current may be uncontrollable without the use of EC due to its singular behavior near edges. All of our comparisons are based on the current values instead of Radar Cross Section (RCS) values. The current values are more sensitive than RCS values in numerical errors but they are not used commonly in the accuracy comparison in Nyström method.

ACKNOWLEDGMENT

This work is partially sponsored by AFOSR MURI grant FA9550-04-1-0326.

REFERENCES

1. Kot, J. S., "Solution of thin-wire integral equations by Nyström methods," *Microw. Opt. Tech. Lett.*, Vol. 3, No. 11, 393–396, 1990.
2. Canino, L. F., J. J. Ottusch, M. A. Stalzer, J. L. Visher, and S. Wandzura, "Numerical solution of the Helmholtz equation in 2D and 3D using a high-order Nyström discretization," *J. Comput. Phys.*, Vol. 146, 627–663, 1998.
3. Gedney, S. D., "On deriving a locally corrected Nyström scheme from a quadrature sampled moment method," *IEEE Trans. Antennas Propagat.*, Vol. 51, No. 9, 2402–2412, 2003.
4. Bouwkamp, C., "A note on singularities occuring at sharp edges in electromagnetic diffraction theory," *Physica*, Vol. 12, 467, 1946.
5. Meixner, J., "The behavior of electromagnetic fields at edges," *IEEE Trans. Antennas Propagat.*, Vol. AP-20, No. 4, 442–446, 1972.
6. Faraji-Dana, R. and Y. Chow, "Edge condition of the field and

a.c. resistance of a rectangular strip conductor," *IEE Proceedings*, Vol. 137, Pt. H, No. 2, Apr. 1990.

7. Lavretsky, E. L., "Taking into account the edge condition in the problem of scattering from the circular aperture in circular-to-rectangular and rectangular-to-rectangular waveguide junctions," *IEE Proc.-Microw. Antennas Propag.*, Vol. 141, No. 1, Feb. 1994.
8. Balanis, C. A., *Advanced Engineering Electromagnetics*, 2nd edition, Wiley, New York, 1989.
9. Abramowitz, M. and I. A. Stegun, *Handbook of Mathematical Functions with Formulas, Graphs and Mathematical Tables*, Dover, New York, 1964.
10. Liu, K. and C. A. Balanis, "Simplifed formulations for two-dimensional TE-polarization field computations," *IEEE Trans. Antennas Propagat.*, Vol. 39, No. 2, 259–262, Feb. 1991.
11. Tong, M. S. and W. C. Chew, "A higher-order Nyström scheme for electromagnetic scattering by arbitrarily shaped surfaces," *IEEE Antennas and Wireless Propagation Letters*, Vol. 4, 277–280, 2005.
12. Stroud, A. H. and D. Secrest, *Gaussian Quadrature Formulas*, Prentice-Hall, Englewood Cliffs, 1966.
13. Ma, J.-H., V. Rokhlin, and S. M. Wandzura, "Generalized Gaussian quadrature rules for systems of arbitrary functions," *SIAM J. Numerical Anal.*, Vol. 33, No. 3, 971–996, Jun. 1996.
14. Press, W. H., B. P. Flannery, S. A. Teukolsky, and W. T. Vetterling, *Numerical Recipes, The Art of Scientific Computing*, Cambridge University Press, Cambridge, 1987.
15. Dwight, H. B., *Tables of Integrals and Other Mathematical Data*, 4th edition, Macmillan, New York, 1961.